Aberystwyth University

Defining key metabolic roles in osmotic adjustment and ROS homeostasis in the recretohalophyte Karelinia caspia under salt stress

Guo, Qiang; Han, Jiwan; Li, Cui; Hou, Xincun; Zhao, Chunqiao; Wang, Qinghai; Wu, Juying; Mur, Luis

ORIGINAL ARTICLE

Physiologia Plantarum

Defining key metabolic roles in osmotic adjustment and ROS homeostasis in the recretohalophyte *Karelinia caspia* under salt stress

Qiang Guo[1] | Jiwan Han[2] | Cui Li[1] | Xincun Hou[1] | Chunqiao Zhao[1] | Qinghai Wang[1] | Juying Wu[1] | Luis A. J. Mur[2,3]

[1]Institute of Grassland, Flowers, and Ecology, Beijing Academy of Agriculture and Forestry Sciences, Beijing, China

[2]College of Software, Shanxi Agricultural University, Taigu, China

[3]Institute of Biological, Environmental, and Rural Sciences, Aberystwyth University, Aberystwyth, UK

Correspondence
Juying Wu, Institute of Grassland, Flowers and Ecology, Beijing Academy of Agriculture and Forestry Sciences, Beijing 100097, China.
Email: wujuying@grass-env.com

Luis A. J. Mur, Institute of Biological, Environmental and Rural Sciences, Aberystwyth University, Aberystwyth, SY23 3DA, UK.
Email: lum@aber.ac.uk

Abstract

The recretohalophyte *Karelinia caspia* is of forage and medical value and can remediate saline soils. We here assess the contribution of primary/secondary metabolism to osmotic adjustment and ROS homeostasis in *Karelinia caspia* under salt stress using multi-omic approaches. Computerized phenomic assessments, tests for cellular osmotic changes and lipid peroxidation indicated that salt treatment had no detectable physical effect on *K. caspia*. Metabolomic analysis indicated that amino acids, saccharides, organic acids, polyamine, phenolic acids, and vitamins accumulated significantly with salt treatment. Transcriptomic assessment identified differentially expressed genes closely linked to the changes in above primary/secondary metabolites under salt stress. In particular, shifts in carbohydrate metabolism (TCA cycle, starch and sucrose metabolism, glycolysis) as well as arginine and proline metabolism were observed to maintain a low osmotic potential. Chlorogenic acid/vitamin E biosynthesis was also enhanced, which would aid in ROS scavenging in the response of *K. caspia* to salt. Overall, our findings define key changes in primary/secondary metabolism that are coordinated to modulate the osmotic balance and ROS homeostasis to contribute to the salt tolerance of *K. caspia*.

1 | INTRODUCTION

Salinization is a serious environmental problem in arid and semi-arid regions, which restricts crops productivity and disrupts ecosystem functions (Tang et al., 2015; Yang et al., 2019a). Global food requirements are expected to increase by 70–110% by 2050 to meet the needs of the rapidly growing human population (Munns et al., 2012), but most crops are very sensitive to high salt, causing osmotic stress and disrupting ion homeostasis (Munns & Tester, 2008). However, halophytes have evolved various mechanisms to ensure their survival and to complete their life cycle in high salt environments (Flowers & Colmer, 2008). They can be used not only in the improvement of saline soils (remediation) but also a promising source of food, fiber, and medicine (Flowers & Muscolo, 2015; Song & Wang, 2014). Therefore, understanding the mechanisms employed by

halophytes to adapt to environmental stresses could be important in breeding programs to improve the salt tolerance of crops (Cui et al., 2020).

The tolerance of plants to salt depends on ion homeostasis, synthesizing metabolites involved in osmotic adjustment and activating antioxidant defense systems (Isayenkov & Maathuis, 2019). One of the effective adaptive strategies in halophytes is the preferential transport of Na^+ into the shoots, where it is compartmentalized into the vacuoles to maintain a low osmotic potential and ion homeostasis under high salinity (Guo et al., 2020a; Shabala, 2013). However, vacuoles become saturated if subjected to long-term high salinity, resulting in the retention of Na^+ in the cytoplasm, which affects the osmotic balance, inhibits metabolic processes and generates excessive ROS (reactive oxygen species; Flowers et al., 2015; Yuan et al., 2015). To counter this, elevated levels of primary metabolites (PMs) in the cytosol can aid to stabilize the internal osmotic potential, strengthen the thermodynamic stability of folded proteins, and protect macromolecular structures by reducing ROS accumulation (Slama et al., 2015; Yancey, 2005). For example, the very high salt tolerance of *Suaeda salsa* could be linked to the higher level of branched-chain amino acids and saccharides in leaves compared with the less tolerant halophyte *Salicornia europaea* (Wang et al., 2021). In the halophyte *Limonium albuferae*, fructose and glucose accumulated, accompanied by a steady level of citric and malic acid, compared with the more salt sensitive *L. doufourii* (González-Orenga et al., 2019). In recretohalophytes, salt is secreted from glands to improve salt tolerance. However, under high salt, recretohalophytes with epidermal bladder cells (EBC), such as *Chenopodium quinoa*, can accumulate more metabolites, including proline, γ-aminobutyric acid (GABA) and inositol, to modulate ion transport than non-EBC (Kiani-Pouya et al., 2017).

Besides a role of PMs in salt responses, a significant contribution is made by secondary metabolites (SMs). Thus, such as tocopherol, phenolic acids and flavonoids, derived from the shikimate pathway, can contribute as nonenzymatic antioxidants (Muñoz & Munné-Bosch, 2019; Sirin & Aslım, 2019). For example, the overexpression of γ-*TMT* (γ-*TOCOPHEROL METHYLTRANSFERASE*), gene coding for a key enzyme of tocopherol biosynthesis, increased the α-tocopherol (vitamin E) content, hence contributing to decreased ROS, lipid peroxidation and ion leakage, conferring salt tolerance to the transgenic tobacco (Jin & Daniell, 2014). In honeysuckle (*Lonicera japonica*), the accumulation of leaf phenolic acids, including chlorogenic acid and luteolosid, suppressed the overproduction of ROS upon salt treatment (Yan et al., 2017). Similarly, β-carotene, vitamin C, phenolic acids, and flavonoids were significantly increased by salt treatment, and acted as ROS scavengers in *Amaranthus tricolor* (Sarker & Oba, 2018). Such observations indicate a coordinated action of PMs and SMs as osmoprotectants and ROS scavengers to balance the osmotic pressure and control ROS overproduction when plants are subjected to salt stress. However, little is known about these mechanisms in the salt tolerance of recretohalophytes.

Karelinia caspia is a recretohalophyte, perennial herb Asteraceae mainly distributed in semi-desert areas and desert grassland in northwestern China and shows strong adaptability to salinity, drought, and

high temperature (Zhang et al., 2014). It is not only an essential forage species for livestock in desert grasslands, but also a pioneer species that plays a crucial role in the improvement of saline soils and desertification control (Wang et al., 2013; Zhang et al., 2020). A previous study showed that the tonoplast Na^+/H^+ antiporter (KcNHX1) mediated Na^+ compartmentalization into the leaf vacuoles to maintain a low osmotic potential in the cytosol, avoiding Na^+ toxicity under salt stress (Liu et al., 2012). Further, the plasma membrane Na^+/H^+ antiporter (KcSOS1) is a key systemic regulator of Na^+ secretion by salt glands; it maintains K^+/Na^+ homeostasis via modulating the Na^+ transport and K^+ uptake/transporter system (Guo et al., 2020b). Other adaptive mechanisms of *K. caspia* to high-salt environment need to be explored, particularly the possible roles of PM and SM changes. These would be especially relevant when salt crystals are deposited on the leaf surface from salt glands, as this would trigger leaf dehydration inducing intracellular oxidative damage. However, leaves of *K. caspia* do not show any sign of dehydration, possibly due to de novo synthesis of organic osmolytes facilitating the osmotic cellular adjustment (Shabala et al., 2014). Moreover, *K. caspia*, as a traditional Chinese medicinal herb, contained bioactive compounds, for example, phenylpropanoid glycosides, triterpenoids, sterols, and flavonoids (He et al., 2016; Yang et al., 2019b), implying that these could be potential ROS scavengers to be contributed to salt tolerance.

Therefore, we predicted that coordinated changes in PM and SM are important in the ability of *K. caspia* to cope with salt stress. In this current study, we identify differentially accumulated metabolites (DAMs), which relate to differentially expressed genes (DEGs) in leaves. Our results confirmed that changes in PM (starch and sucrose metabolism, TCA cycle, glycolysis, arginine and proline metabolism) and SM (chlorogenic acid- and vitamin E biosynthesis) contribute to the osmotic adjustment and ROS scavenging taking place in *K. caspia* exposed to salinity stress. These findings could be important for the exploitation of *K. caspia* in saline soil remediation.

2 | MATERIALS AND METHODS

2.1 | Plant materials and growth conditions

A single accession of *Karelinia caspia* (designated Guo1) was used as described by Guo et al. (2020b). The seeds were sown on black plastic tray containing John Innes No. 1 compost and sand (v/v, 4:1) under a daily photoperiod of 16/8 h (light/dark) at 24/20°C, relative humidity of 50–60% and 300–400 μmol $m^{-2} s^{-1}$ photosynthetically active radiation in a growth chamber (Conviron, UK). The seedlings were selected for uniformity after 2 weeks, they were then transferred into plastic pots and irrigated every 2 days with tap water for 3 weeks. Our previous study showed that *K. caspia* plants grow well on 200 mM NaCl compared with control plants (Guo et al., 2020b); therefore, 5-week-old seedlings were watered with 0 or 200 mM NaCl for 2 days. All seedlings were grown in the same growth chamber. The pots were arranged in a randomized block design. After a 2-day exposure period, shoots were harvested and washed thoroughly with tap water followed by

deionized water. Samples were then oven-dried at 80°C to a constant dry weight (DW). The relative growth rate (RGR) was calculated using the formula RGR = (lnWj − lnWi)/Δt, where Wj and Wi are final and initial total DW, respectively, and Δt is the time elapsed (days) between the two measurement (Martínez et al., 2005).

2.2 | Measurements of chlorophyll fluorescence, imaging, and feature extraction

Chlorophyll fluorescence was performed at room temperature using a Handy-PEA (Hansatech Instruments). Leaf surfaces were dark-adapted for 30 min using dark leaf clips before measurements. After dark adaptation, the maximum quantum efficiency of PSII photochemistry (F_v/F_m) was instantly measured on leaf surface using a photosynthetic photon flux density of 3000 µmol m^{-2} s^{-1} as saturating flash for the duration of 1 s, where F_v was the difference between F_m and F_0 (Sharma et al., 2015). For imaging and feature extraction, we captured the images before and after treatment using a camera, and exported them as RGB color images. Subsequently, the images were processed to extract features data including height and pixel values (green) according to C++ and OpenCV 2.4.9, an open-source computer vision library (Fisher et al., 2016).

2.3 | Measurements of water potential, osmotic potential, and turgor pressure in leaf

The PSYPRO water potential system (C-52 Sample Chamber, WESCOR Inc.) was used to measure the leaf water potential (Ψw, MPa) based on the manufacturer's instructions. Leaf osmotic potential (Ψs) measurements were performed using the method described by Ma et al. (2012). In brief, fresh leaf samples were quickly frozen in liquid nitrogen and slowly thawed. A syringe was used to collect cell sap that was subsequently centrifuged at 9000g for 5 min. The osmolality (n, mmol kg^{-1}) of the supernatant was recorded using a freezing point osmometer (Osmomat3000, Gonotec GmbH) at room temperature (25°C). The readings (n) were used to calculate the Ψs (MPa) with the van't Hoff equation as -nRT, where R is the gas constant (0.008314 m^3 MPa mol^{-1} K^{-1}) and T is the thermodynamic temperature (298.8 K). Leaf turgor pressure (Ψt, MPa) was calculated using the equation: $\Psi t = \Psi w - \Psi s$ (Cui et al., 2020).

2.4 | Determination of chlorophyll, lipid peroxidation, hydrogen peroxide, and antioxidant enzymes

Five hundred milligrams of fresh leaves was ground to powder in liquid nitrogen with a mortar and pestle. Analyses of leaf chlorophyll (Chl), malondialdehyde (MDA), hydrogen peroxide (H_2O_2) and the activity of superoxide dismutase (SOD, EC1.15.1.1) and peroxidase (POD, EC 1.11.1.7) were performed according to the methods in Guo et al. (2017). The activity of catalase (CAT, EC 1.11.1.6) was analyzed

by measuring the residual H_2O_2 based on the method of Liao et al. (2019) and recorded at 240 nm every 1 min during 5 min. All optical density of reaction supernatant was measured using a UV2600 spectrophotometer (Techcomp). Each treatment was replicated six times, with two pooled plants per replicate.

2.5 | Determination of cations concentration

Dried leaves and roots were ground and digested in a mixture of HNO$_3$/HClO$_4$ (5/1, v/v) for 24 h and then heated at 150–200°C to near dryness. After cooling, the residue was dissolved in distilled deionized water to a total volume of 25 ml. Na$^+$, K$^+$, and Ca^{2+} concentrations were determined using an atomic absorption spectrophotometer (AA-6300C, Shimadzu).

2.6 | RNA isolation, library construction, and sequencing

Total RNA was extracted from six samples using a plant RNA purification reagent (Invitrogen) according to the manufacturer's instructions. DNase I (Invitrogen) was added, and incubated at 37°C for 15 min to remove genomic DNA contamination. The concentration and quality of purified RNA was measured using the NanoDrop2000 Spectrophotometer (Thermo Scientific) and the Bioanalyzer 2100 system (Agilent Technologies), respectively. 1 µg of total RNA was used to construct a RNA sequencing (RNA-seq) library using TruSeq RNA Sample Prep Kit according to the manufacturer's instructions (Illumina). The samples were sequenced on the Illumina HiSeq 2500 platform at Shanghai Majorbio Bio-pharm Technology Co., Ltd.

2.7 | De novo assembly and functional annotation

Raw reads were assessed by quality score using the Fastx_Toolkit (http://hannonlab.cshl.edu/fastx_toolkit/, version 0.0.14). Raw reads were trimmed and low-quality reads removed using Seqprep (https://github.com/jstjohn/SeqPrep) and Sickle (https://github.-com/najoshi/sickle). The raw data has been deposited in the National Center for Biotechnology Information (NCBI) Sequence Read Archive under the accession number PRJNA744046.

De novo assembly of the clean reads was done using the paired-end method of Trinity (https://github.com/trinityrnaseq/trinityrnaseq), and the derivation of unigenes was performed according to the method described by Blande et al. (2017). For gene functional annotations, all of the unigenes were aligned to six protein databases, Nr (NCBI nonredundant protein), Swiss-Prot (Swiss-Prot protein database), Pfam (Protein family), GO (Gene Ontology terms), COGs (Clusters of Orthologous Groups), and KEGG (Kyoto Encyclopedia of Genes and Genomes), using the BLASTX algorithm, with an E value threshold of 10^{-5} (Dong et al., 2014).

2.8 | Differentially expressed genes (DEGs) and enrichment analysis

Gene expression was calculated by mapping clean reads to the unigenes database using the RSEM software package (Li & Dewey, 2011). The TPM (transcripts per million reads) method was used to normalize and quantify the expression levels of unigenes (Xue et al., 2010). The analysis of DEGs was performed by DESeq2 software under the standard parameter of the p value <0.05 and $|\log_2 (FC)|$ >1 (Love et al., 2014). The BH (FDR correction with Benjamini/Hochberg) method was used to adjust p value. The identified DEGs were uploaded into the Majorbiol Cloud Platform (https://cloud.majorbio.com/) to analyze the expression differences, and GO terms/KEGG pathway enrichment according to FDR <0.05.

2.9 | qRT-PCR validation of candidate DGEs expression

Total RNA was extracted from leaves as described above. cDNA synthesis was conducted using a ×5 Primescript RTase mix (Takara, Biotech Co.). Quantitative real-time RT-PCR (qRT-PCR) was performed on a thermal cycler (CF96X, Bio-Rad) with the primers described in Table S1 and SYBR Green PCR (Takara Biotech Co.) as a master mix. *KcACTIN* was used as a reference gene for RNA normalization and was amplified in parallel with the target genes (Zhang et al., 2020). Relative expression levels were derived based on the $2^{-\Delta\Delta Ct}$ method (Guo et al., 2020b). Each experiment was carried out on three biological replicates.

2.10 | Extraction and profiling of metabolites

The metabolite was extracted from leaves sample according to Paes de Araújo et al. (2019) with minor modifications. Briefly, approximately 50 mg of leaf was harvested in 2 ml microcentrifuge tube, and immediately frozen in liquid nitrogen. The frozen sample was ground into a powder with a sterile stainless steel ball for 30 s at 30 Hz using the oscillating mill MM200 (Retsch), then returned to the ice. 1 ml of prechilled chloroform: methanol: water (v/v/v, 1: 2.5: 1) was added into each sample, vortexed, then shaken at 4°C for 20 min, followed by microcentrifuging at 21,000 g for 6 min at 4°C. 100 μl of supernatant was transferred into a glass vial and capped for subsequent flow injection electrospray ionization high resolution-mass spectrometry (FIE-HRMS). Each treatment was performed six times (one independent leaf sample in each replicate).

FIE-HRMS was performed using Q-Exactive plus mass analyzer instrument with ultra-high pressure liquid chromatography system (Thermo Fisher Scientific), where mass-to-charge ratios (m/z) were generated in positive (POS) and negative (NEG) ionization mode in a single run as described by Beckmann et al. (2008) and Baptista et al. (2018). The scanning ranges were from 55–280 to 270–1200 in both POS and NEG ionization mode. Signals were normalized to total ion count. All metabolomics data assessed using MetaboAnalyst

(version 5.0) software (Pang et al., 2021). In brief, data were filtered by interquantile range, $\log_{10}$ transformed and Pareto scaled. Student t-test was used to identify the significant m/z, which was uploaded into the specific module (MS peaks to pathways) to match potential metabolites using the mummichog algorithm and interrogation of KEGG and MZedDB (http://maltese.dbs.aber.ac.uk:8888/hrmet/index.html) databases based on 5 ppm thresholds and considering various ionization forms of metabolite feature. Correlation analyses, PCA, hierarchical cluster analyses and debiased sparse partial correlation (DSPC) analyses were performed using the R-based platform MetaboAnalyst 5.0 (Pang et al., 2021).

2.11 | Statistical analysis

For the physiological parameters analyses, each treatment was repeated six times, each replicates consisting of a pool of three plants. Data are presented as means with SD. Data analyses, including one-way ANOVA and Duncan's multiple range tests, were performed by SPSS version 23.0 software (IBM SPSS statistics, SPSS Inc.).

3 | RESULTS

3.1 | Assessing the phenotypic, physiological, and biochemical responses to salt in *K. caspia*

The impact of salt stress on the growth and photosynthesis parameters was determined in *K. caspia* in response to control (0 mM NaCl) and salt (200 mM NaCl) treatments after 2 days. Compared with the control, salt treatment had no impact on the phenotypic features (height and color) based on RGB image analyses (Figure 1A–C). No marked differences were observed in relative growth rate (RGR) between control and salt (Figure 1D). The absence of effects was also seen in total Chl content, Chl a/b, chlorophyll fluorescence parameters (Figure 1E–F and Table S2). These data confirmed that *K. caspia* exhibits good salt tolerance.

To further examine the salt-induced oxidative stress in *K. caspia*, the accumulation of the membrane lipid peroxidation biomarker malondialdehyde (MDA) as well as H_2O_2 and antioxidant enzyme activities were assessed. There were no significant differences in MDA or H_2O_2 content between the leaves of the control and salt-treated plants (Table 1). However, the addition of 200 mM NaCl increased the activities of SOD, POD, or CAT, which were 1.43-, 1.88-, or 1.77 fold higher, respectively, than that of controls (Table 1). This suggests that enhanced antioxidant activities protect against the salt-induced oxidative stress.

3.2 | Ions accumulation and osmotic adjustment in salt-treated *K. caspia*

To assess the impact of salt stress on induced ionic imbalance, Na^+, K^+, and Ca^{2+} concentrations were measured in *K. caspia* submitted to
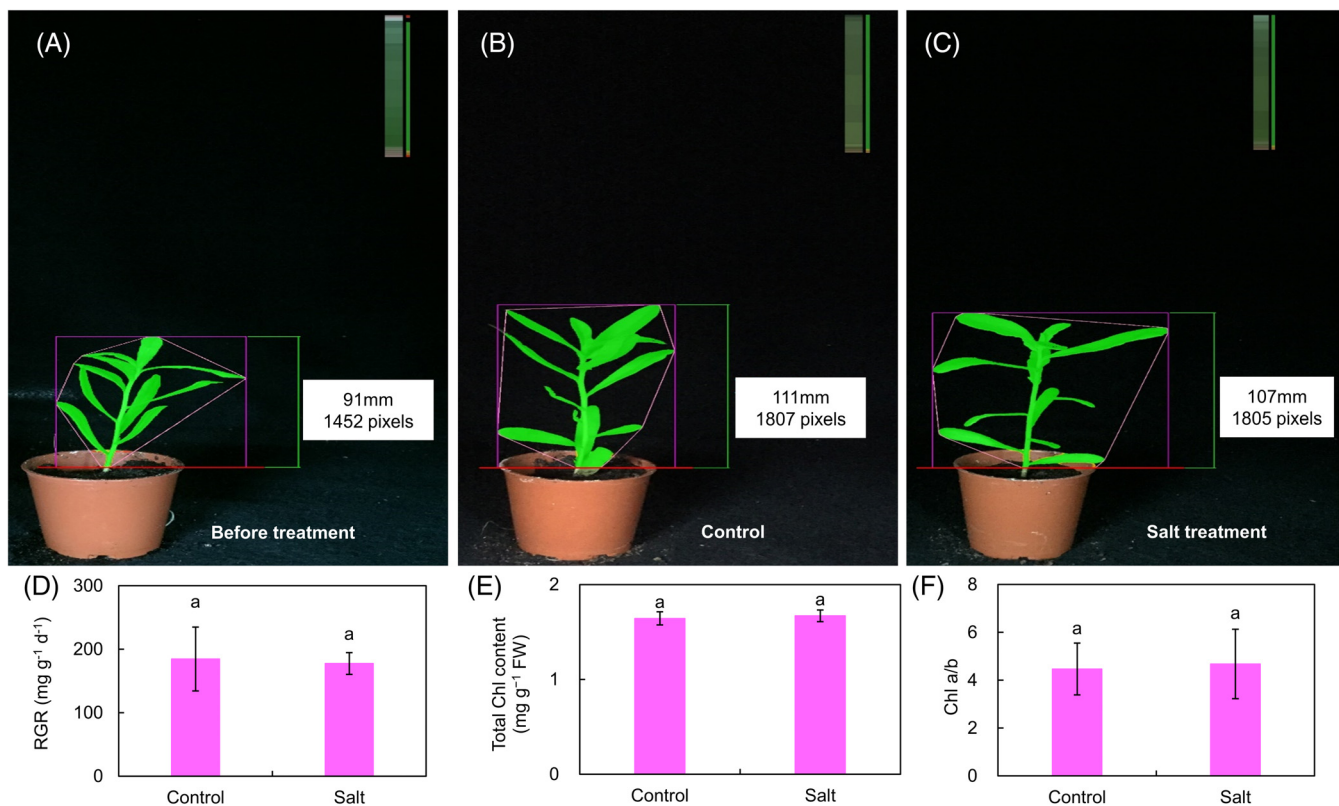
FIGURE 1 (A–C) *Karelinia caspia* phenotypic features (height and color) before treatment, and after 2 days at the control or salt treatment. Each pixel number reflects the side projective area of each plant and therefore increases with plant biomass. The color bars show the color distribution of the plants. The control and salt treatment plants have higher green color percentage. (D) Analyses of relative growth rate (RGR), (E) total chlorophyll (Chl) content, and (F) Chl *a/b* in *K. caspia* seedlings under control and salt conditions. Data are means ± SD ($n = 6$ independent plants). Different letters indicate significant differences at p <0.05 (Duncan's test)

TABLE 1 Effect of salt treatment on lipid peroxidation, H_2O_2 accumulation, and the activity of SOD, POD, and CAT in the leaves of *K. caspia*

NaCl treatment (mM)	MDA content (μmol g^{-1} FW)	H_2O_2 content (μmol g^{-1} FW)	SOD activity (U g^{-1} FW)	POD activity (U g^{-1} min^{-1} FW)	CAT activity (U g^{-1} min^{-1} FW)
0	0.21 ± 0.058a	0.77 ± 0.07a	60.28 ± 7.16b	16.67 ± 3.72b	125 ± 28.87b
200	0.24 ± 0.042a	0.81 ± 0.087a	86.07 ± 7.64a	31.33 ± 6.89a	221.33 ± 46.33a

Note: Data are means ± SD ($n = 6$ independent plants). Different letters indicate significant differences at $p < 0.05$ (Duncan's test).

salt treatment for 2 days. Under the control conditions, there was no difference in Na$^+$, K$^+$, or Ca^{2+} concentrations between leaf and root (Figure 2). Conversely, Na$^+$ concentrations were greatly increased in both leaves and roots under salt treatments relative to the controls (Figure 2A). However, no significant differences were found in K$^+$ or Ca^{2+} in leaves between the controls and salt treatments (Figure 2B,C), indicating that *K. caspia* could maintain a constant K$^+$ and Ca^{2+} concentrations under salt stress.

We then estimated the effect of salt on osmotic adjustments within the leaves of *K. caspia* (Figure 2D–F). Salt treatment markedly decreased leaf Ψw and Ψs, but significantly enhanced leaf Ψt in comparison with the controls. These data demonstrated that *K. caspia* could accumulate osmolytes, including inorganic salts and organic solutes (metabolites), to improve the hydration and turgor pressure in the leaf.

3.3 | Metabolomic analysis in the leaf of *K. caspia* response to salt stress

Metabolomics assessments were based on the use of FIE-HRMS. The derived data were assessed using PCA, which showed a clear separation between control and salt-treated *K. caspia* leaves with PC1 explaining 63% of the total variation (Figure 3A). The major sources of variation were further determined using *t*-tests and corrected for false discovery rates (FDR). A total of 66 DAMs were subsequently identified based on accurate mass, isotope and ionization patterns. Most DAMs were primary metabolites (i.e., amino acids, amines, organic acids, and carbohydrates) except a plant hormone (salicylic acid, SA), vitamins (α-tocopherol, γ-tocopherol, and thiamine) and some secondary metabolites (betaine, caffeic acid, chlorogenic acid, *p*-coumaric acid, *p*-coumary CoA, 4-coumaryl shikimic acid, and *p*-coumaryl quinic
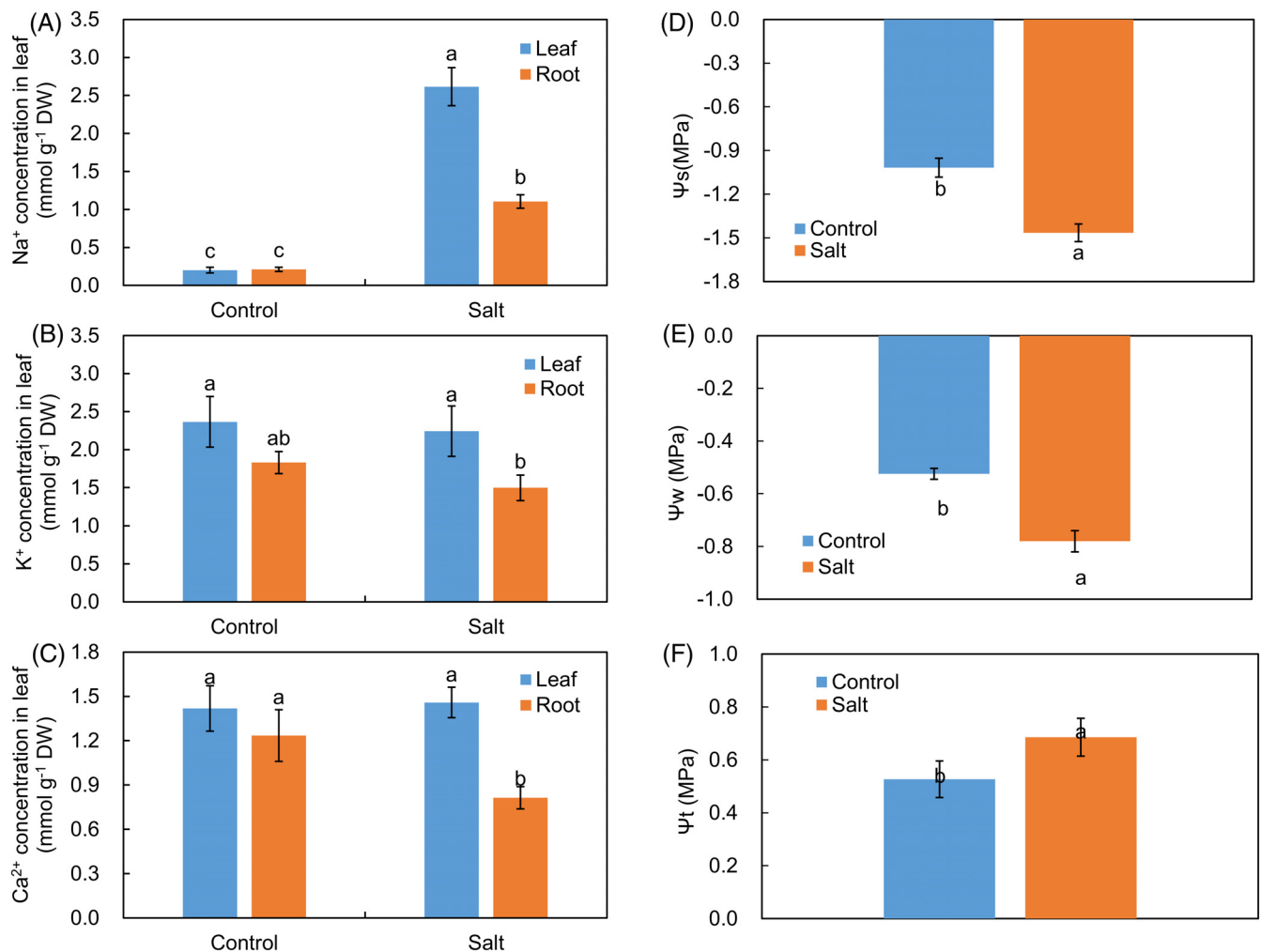
FIGURE 2   Effect of the control and salt treatment on tissue's Na$^+$ (A), K$^+$ (B), and Ca^{2+} (C) concentration and (D) leaf osmotic potential (Ψs), (*E*) leaf water potential (Ψw), and (*F*) leaf turgor pressure (Ψt) in *K. caspia*. Data are means ± SD (*n* = 6, independent plants). Different letters indicate significant differences at *p* <0.05 (Duncan's test)

acid). When displayed using a heatmap, 50 and 16 DAMs were up- and downregulated under salt stress, respectively, compared with the control group (Figure 3B).

To investigate the metabolic pathways involved in *K. caspia* exposed to salt stress, the DAMs were mapped to the Arabidopsis KEGG pathway library. DAMs could be mapped to the following metabolic pathways: citrate cycle (TCA cycle), starch and sucrose metabolism, arginine and proline metabolism, glycolysis/gluconeogenesis, ubiquinone and other terpenoid-quinone biosynthesis, as well as phenylpropanoid biosynthesis based on an FDR <0.05 and impact value >0.2 (Figure 4A). Moreover, there were significant correlations between these DAMs as indicated by debiased sparse partial correlation (DSPC) network analysis (Figure 4B). For example, UDP-glucose was correlated with dextrin, D-glucose 6-phosphate, 4-hydroxyphenylpyruvate, sucrose 6-phosphate, and succinate, implicating UDP-glucose is an important precursor of these metabolites when *K. caspia* is subjected to salt stress.

3.4 | RNA-seq, de novo assembly and functional annotation in the leaf of *K. caspia* under salt stress

To compare these changes with the salt-responsive transcriptome in *K. caspia*, cDNA libraries were constructed from leaves of plants grown in the absence or presence of 200 mM NaCl for 2 days. The libraries were sequenced using the Illumina HiSeq 2500 platform. Control samples generated from 44.3- to 51.5 million clear reads, while 42.2- to 44.8 million clear reads were obtained insalt-treated samples, with Q20 over 98%, Q30 over 95%, and GC content over 45% (Table S3). This indicated that the RNA sequencing output and quality were adequate for further analysis.

A total of 42,678 unigenes were subsequently assembled from the short clean reads using Trinity software. The average unigenes length was 1049.67 bp, 16,772 unigenes had a length over 1000 bp (Table S4). More than 45% of the unigenes were annotated from public protein libraries (NR, SwissProt, Pfam, COG and GO) with a cut-off
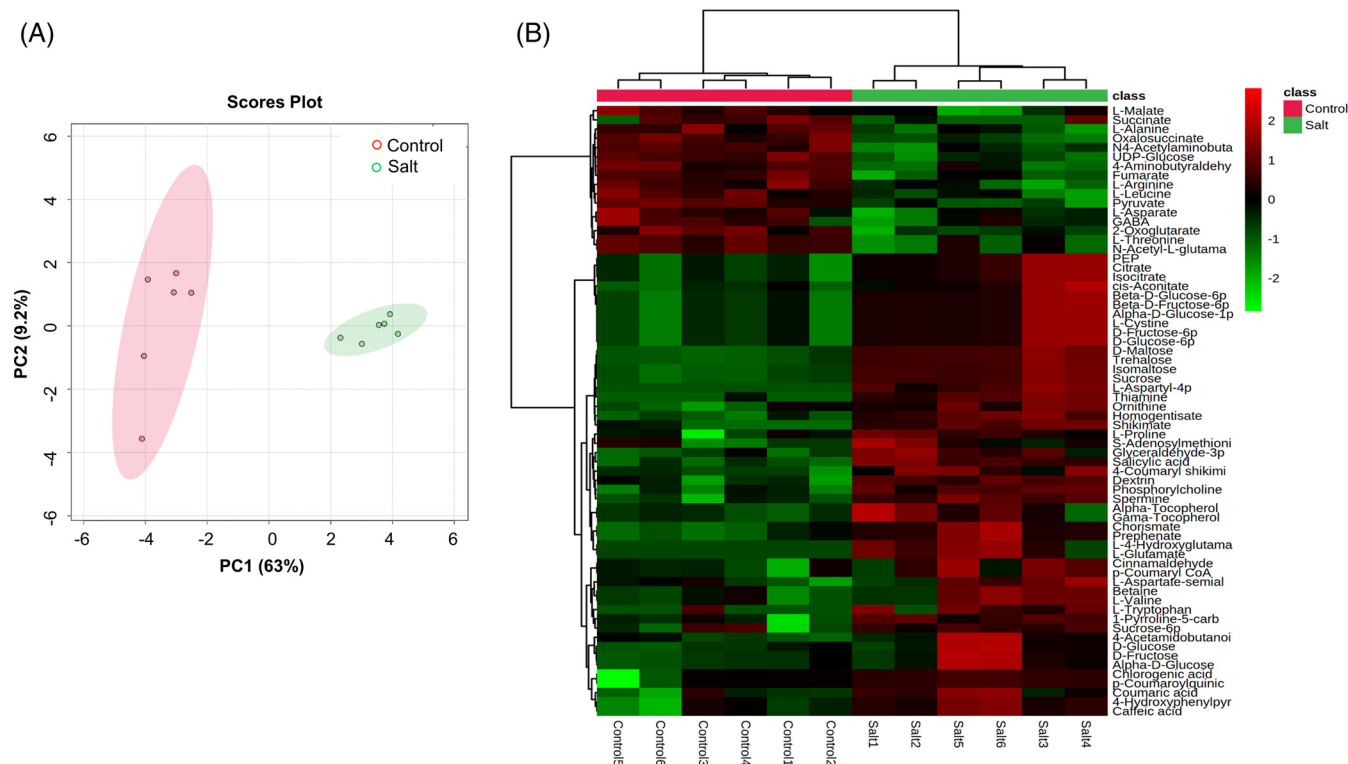
FIGURE 3 Metabolomics analysis of leaves in *K. caspia* exposed to control and salt treatments. (A) Principal component analysis (PCA) of 66 metabolites detected by FIE-HRMS. (B) Heatmap for hierarchical clustering analysis of differentially accumulated metabolites (DAMs) associated with primary and secondary metabolism. The color scale indicates the different $\log_{10}$ (FC) values of DAMs
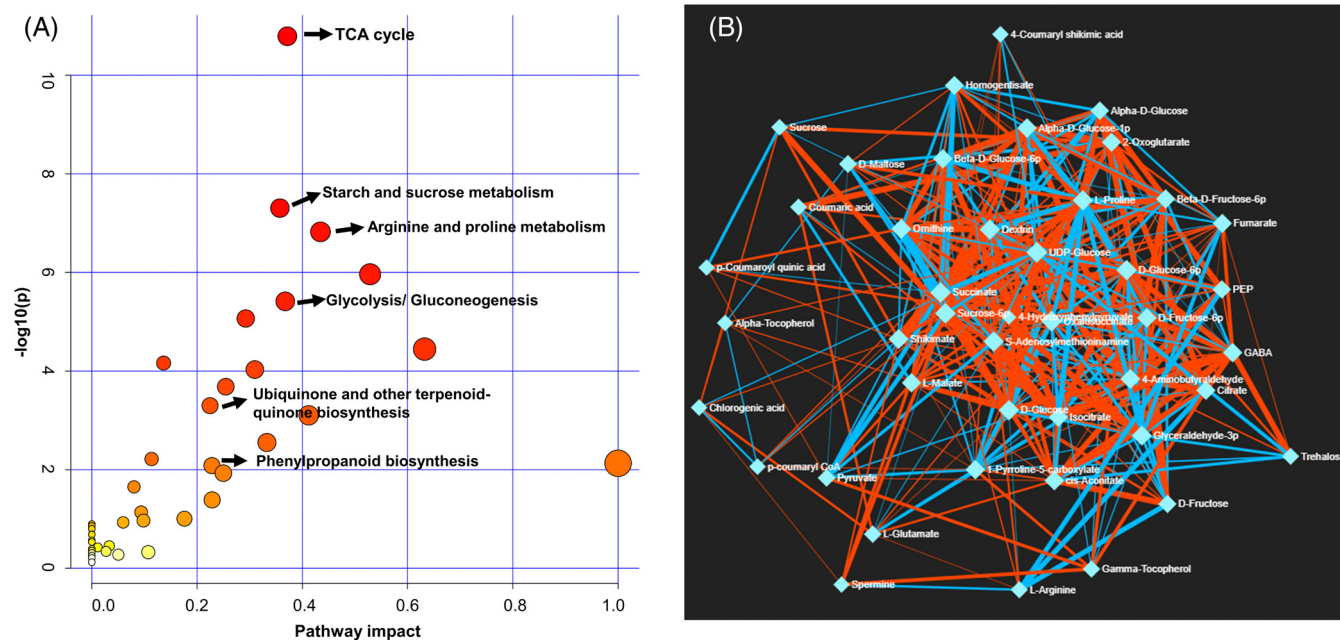
FIGURE 4 Metabolic pathways analysis in *K. caspia* exposed to the control and salt treatment. (A) KEGG pathway analysis based on DAMs. Every circle represents a metabolic pathway, with red or yellow color indicating high or low impact. (B) The interaction relationships between DAMs was analyzed by debiased sparse partial correlation (DSPC) network. Nodes represent metabolites, and edges indicate the correlation between metabolites. Nodes are colored to correspond to their compound classes

(A)

(B)

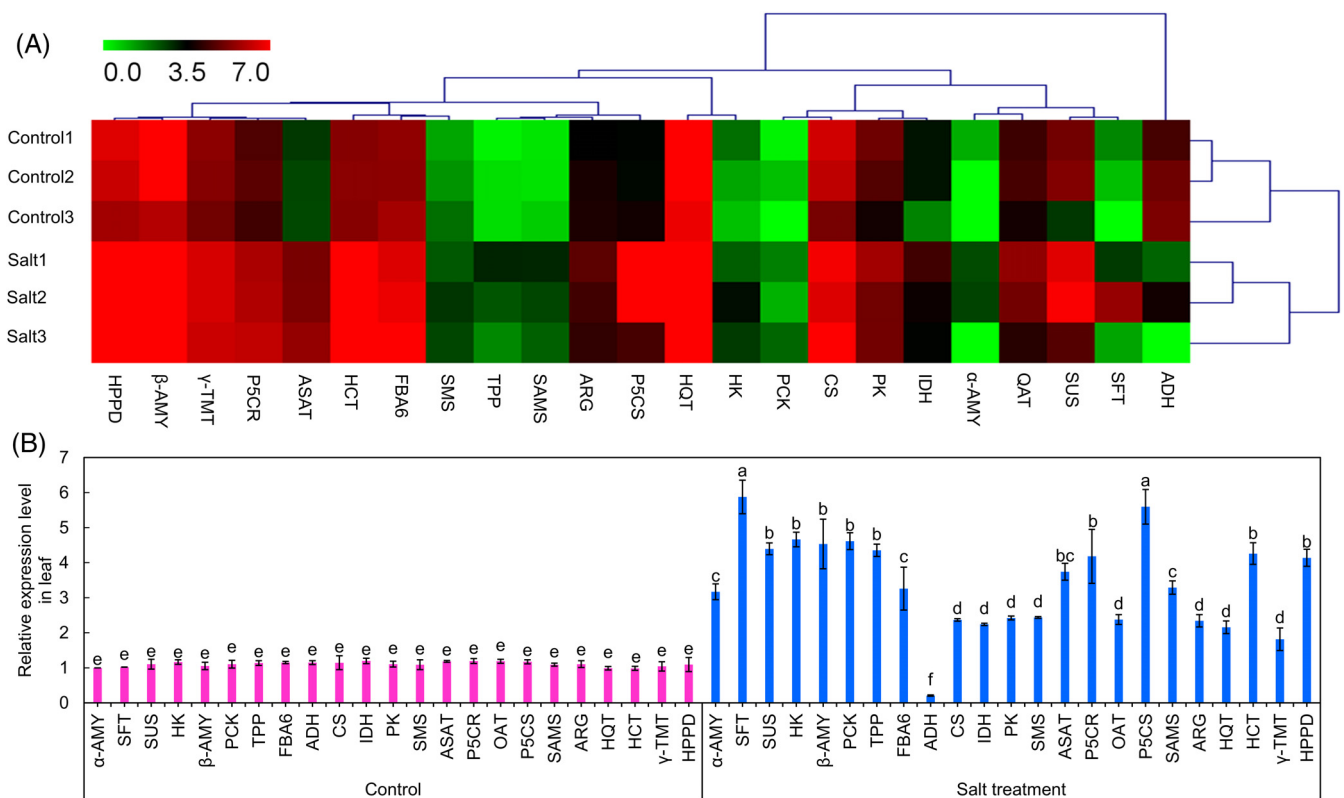**FIGURE 5** Analysis of leaf gene expression profiles in the representative metabolic pathways in *K. caspia* exposed to the control and salt treatment. (A) Hierarchical cluster analysis was performed on data acquired by RNA-seq. Heat map was constructed for TPM of DGEs associated with TCA cycle, starch and sucrose metabolism, arginine and proline metabolism, glycolysis/gluconeogenesis, ubiquinone and other terpenoid-quinone biosynthesis, as well as phenylpropanoid biosynthesis. The color scale represents the upregulated or downregulated genes expression based on the thresholds of *p* value <0.05 and |log$_2$ (FC)| >1. (B) Validation of the expression of the candidate DEGs using qRT-PCR. Data are means ± SD (*n* = 3 independent samples). Different letters indicate significant differences at *p* <0.05 (Duncan's test)

E value of 10^{-5} (Table S5). The remainder could not be annotated as a *K. caspia* reference genome has yet to be generated.

Next, unigenes expression levels and differentially expressed genes (DEGs) between the control and salt-treated groups were defined. Using RSEM software, the unigene expression distribution had a mean maximum and minimum of 4.85 and 1.22 for controls and 4.82 and 0.95 for salt treatment based on counting the transcripts per million (TPM) (Figure S1A). The Venn diagram showed that 19,695 unigenes were co-expressed between the control and salt stress groups (Figure S1B). In line with this, Pearson correlation analysis also indicated some similarity in transcriptome profiles (*r*^{2} = 0.727 to 0.989) between the three replicates of the two sample groups (Figure S1C). Nevertheless, PCA analysis could distinguish between the samples without or with salt treatment (Figure S2A). DEGs were identified between the control and salt-treated groups using DESeq2, with a *p* value <0.05 and log$_2$ (FC)| >1. The volcano plots showed that 2290 or 1939 DEGs were upregulated or downregulated by salt treatment compared with the control group (Figure S2B); they are displayed using a heatmap (Figure S2C).

To further gain insight into the functions of the DEGs underlying salt tolerance, these were linked to GO terms and assessed by KEGG enrichment analyses using the goatools platform. GO annotation

analysis indicated that DEGs were significantly enriched in biological process (BP), cellular component (CC), and molecular function (MF) (Figure S2D). Additionally, KEGG enrichment analyses were conducted to assess the association between DEGs and metabolic pathways in *K. caspia* under salt stress. KEGG enrichment analyses categorized 224 DEGs into 20 pathways. These were related to PM metabolism (amino acids and carbohydrates), plant hormone signal transduction, MAPK signaling, biosynthesis of secondary metabolites, and carbohydrate metabolism (Figure S2E).

3.5 | Correlation analyses of the expression of metabolism-related genes and corresponding metabolites in the leaf of *K. caspia*

To further explore the salt mechanisms of metabolic responses in *K. caspia* at the transcriptome level, we mapped the expression level of genes related to KEGG pathways including carbohydrate metabolism (starch and sucrose metabolism, glycolysis and TCA cycle), arginine, and proline metabolism as well as chlorogenic acid/vitamin E biosynthesis. From the transcriptome data and the KEGG pathway assessment, we focused on genes involved in
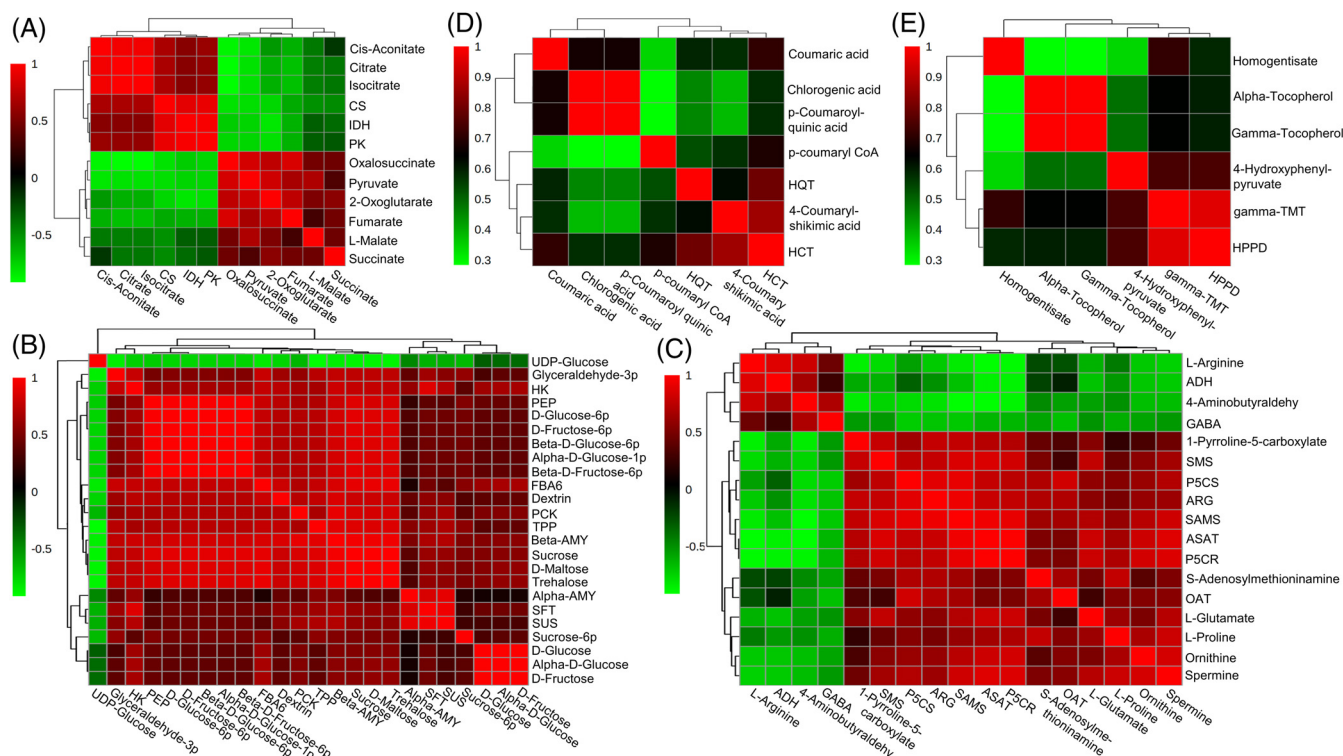
FIGURE 6 Correlation analysis between metabolome and transcriptome in the leaf of *K. caspia* exposed to the control and salt treatment. The heat map shows the correlation coefficient between DEGs and DAMs involved in (A) TCA cycle, (B) starch and sucrose metabolism plus glycolysis/gluconeogenesis, (C) arginine and proline metabolism, (D) phenylpropanoid (chlorogenic acid) biosynthesis, as well as (E) ubiquinone and other terpenoid-quinone (vitamin E) biosynthesis by Pearson's correlation analyses

carbohydrate metabolism that were upregulated by salt compared with controls (Figure 5A): *HK* (*hexokinase*, TRINITY_DN12312_c0_g1), *SFT* (*sucrose 1-fructosyl transferase*, TRINITY_DN9570_c0_g1), *TPP* (*trehalose 6-phosphate phosphatase*, TRINITY_DN8280_c1_g1), *SUS* (*sucrose synthase*, TRINITY_DN8807_c0_g1), *α-AMY* (*α-amylase 1*, TRINITY_DN28863_c0_g1), *β-AMY* (*β-amylase 1*, TRINITY_DN9956_c0_g2), *FBA6* (*fructose-bisphosphate aldolase 6*, TRINITY_DN123_c0_g1), *PCK* (*phosphoenolpyruvate carboxykinase*, TRINITY_DN8290_c0_g1), *CS* (*citrate synthase*, TRINITY_DN4762_c0_g1), *IDH* (*isocitrate dehydrogenase*, TRINITY_DN31728_c0_g1), and *PK* (*pyruvate kinase*, TRINITY_DN1926_c0_g1). Also, key enzymes related to arginine and proline metabolism were all upregulated by salt: *SMS* (*spermine synthase*, TRINITY_DN2782_c0_g4), *SAMS* (*s-adenosylmethionine synthase*, TRINITY_DN29693_c0_g1), *OAT* (*ornithine aminotransferase*, TRINITY_DN16267_c0_g1), *ARG* (*arginase*, TRINITY_DN9521_c0_g1), *P5CR* (*pyrroline-5-carboxylate reductase*, TRINITY_DN16336_c0_g2), *ASAT* (*aspartate aminotransferase*, TRINITY_DN4614_c0_g3), as well as *P5CS* (*delta-1-pyrroline-5-carboxylate synthase*, TRINITY_DN14855_c0_g1). Of the genes examined, only *ADH* (*aldehyde dehydrogenase*, TRINITY_DN1085_c0_g1) was downregulated (Figure 5A). Furthermore, salt stress elevated the expression level of *HQT* (hydroxycinnamoyl-CoA: quinate hydroxycinnamoyl transferase, TRINITY_DN7710_c0_g2) /*HCT* (hydroxycinnamoyl-CoA: shikimate/quinate hydroxycinnamoyl

transferase, TRINITY_DN6971_c0_g1) and HPPD (hydroxyphenyl pyruvate dioxygenase, TRINITY_DN6847_c0_g2)/γ-TMT (TRINITY_DN14107_c1_g1) involved in the biosynthesis of phenylpropanoid (chlorogenic acid) or ubiquinone and other terpenoid-quinone (vitamin E). These results were all validated by qRT-PCR (Figure 5B).

As expected, the modulation in the expression of these genes correlated with the corresponding metabolite contents (Figure 6). Using the DSPC tool, the changes in enzymes-encoding genes and their corresponding metabolites are visualized (Figure 7), where upregualtions are shown in red and downregualtion in green compared with controls. These data suggested that carbohydrate metabolism (starch and sucrose metabolism plus TCA cycle), proline/spermine biosynthesis, as well as chlorogenic acid/vitamin E biosynthesis are involved in the salt response of *K. caspia*.

4 | DISCUSSION

Karelinia caspia is a forage species and traditional Chinese medicine, which occupies an important place in the North China desert ecosystem by being very salt-tolerant and involved in stabilizing and potentially remediating saline soils. Beyond its Chinese context, it could represent a model system to study the mechanisms of salt tolerance in halophytes. This knowledge could then be used to inform crop
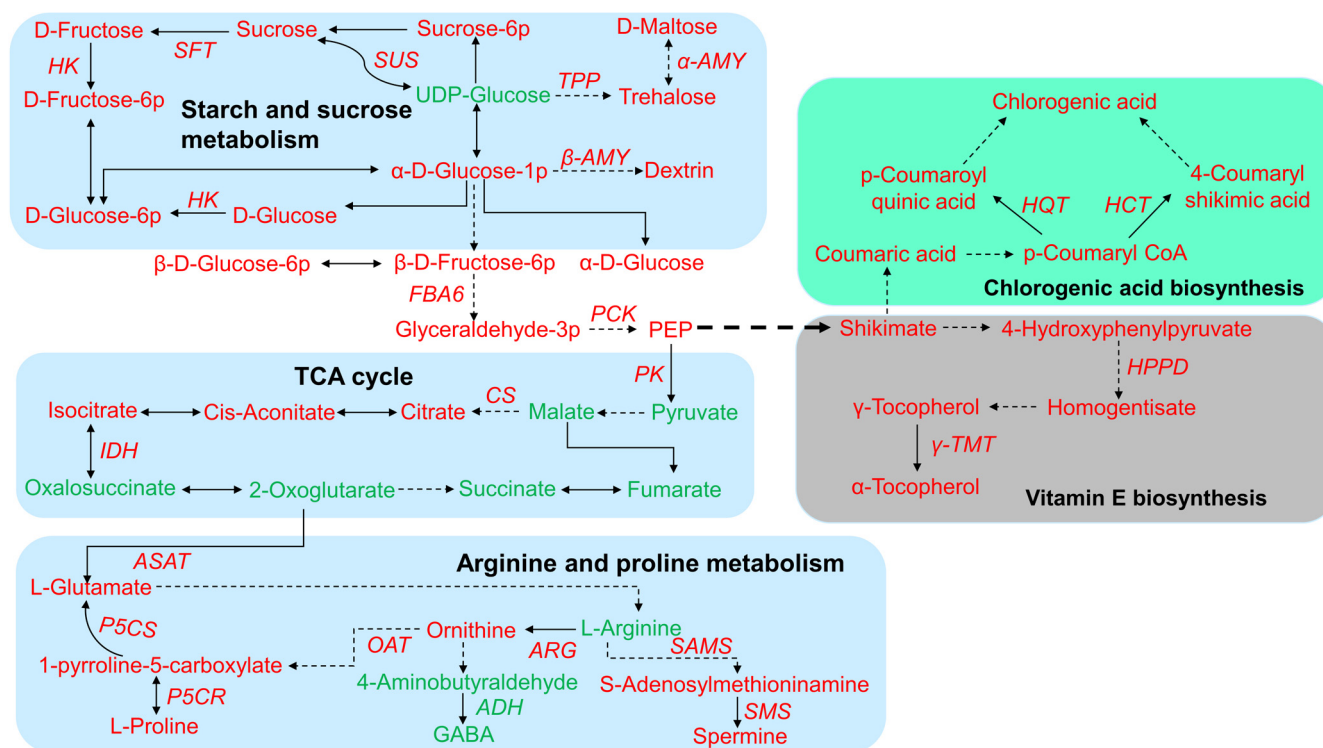
FIGURE 7 Schematic diagram of the changes in expression level of key genes and corresponding metabolites mapped into representative metabolic pathways (starch and sucrose metabolism, glycolysis, TCA cycle, arginine and proline metabolism, chlorogenic acid/vitamin E biosynthesis) in leaf of *K. caspia* exposed to salt. Upright or italics represents metabolites or key enzyme genes. Red or green color shows upregulation or downregulation, respectively, in metabolites and genes

breeding programs. To define the mechanisms of salt tolerance in *K. caspia*, we employed transcriptomic and metabolomic approaches.

4.1 | Saccharide metabolism and proline/spermine biosynthesis facilitate the osmotic adjustment in *K. caspia* under salt stress

Salt stress led to low osmotic potential and high turgor pressure in *K. caspia* leaves (Figure 2). We suggest that the accumulation of organic osmolytes (saccharides, proline, and spermine) and inorganic ions (Figures 2 and 3) facilitated the continued water influx and turgor maintenance under salt conditions (Cui et al., 2020).

Saccharides' metabolism is involved in modulating many physiological processes, including responses to abiotic stresses in plants (Chen et al., 2019). Our data showed that salt treatment upregulated the sucrose content and transcription of *SUCROSE SYNTHASE* (*SUS*) as well as a slight increase in chlorophyll content (Figure 6B and Table S2), suggesting that *SUS* could maintain photosynthesis even in stress conditions as already suggested (Li et al., 2021). We found an increased transcription of *SUCROSE 1-FRUCTOSYL TRANSFERASE* (*SFT*) and fructose concentrations with salt stress (Figure 6B), implying sucrose was converted into fructose to be involved in saccharides metabolism via *SFT*. Meanwhile, the upregulation of *HEXOKINASE* (*HK*) was significantly correlated with the accumulation of glucose,

glucose-6p, fructose, and fructose-6p in our gene-metabolite interaction network (Figure 6B). This reflected the role of hexokinase in hexose phosphorylation to regulate saccharide utilization, hence serving as a sensor for glycolysis of D-glucose and D-fructose (Li et al., 2018). In addition, sucrose synthase converts sucrose into UDP-glucose (UDPG) (Gao et al., 2020) to be further catalyzed into trehalose-6-phosphate (T6P) under trehalose 6-phosphate synthase, followed by T6P was dephosphorylated to trehalose by TPP (Iordachescu & Imai, 2008). In line with this, the transcriptional and metabolite components of sucrose flux to trehalose were significantly activated upon salt treatment in our study (Figure 7). This agreed with the role of trehalose as an established compatible solute in osmotic adjustment and protein/membrane protectant under abiotic stress (Elbein et al., 2003).

Proline is an organic osmolyte that has an important osmoprotective role in cells and also enhances the ability of antioxidant enzymes to remove ROS during salt stress (Ghahremani et al., 2014). It seems likely that the biosynthesis and accumulation of proline are affected in *K. caspia* by salt as we observed salt-upregulated *ASAT/P5CS/OAT/P5CR* expression and the corresponding metabolites (glutamate/1-pyrroline-5-carboxylate/ornithine/proline) (Figure 6C). 2-oxoglutarate is an important precursor of the biosynthesis of glutamate via aspartate aminotransferase (Singh et al., 2016). Glutamate is reduced to L-glutamate-5-semialdehyde by delta-1-pyrroline-5-carboxylate synthetase, which is further converted into

1-pyrroline-5-carboxylate (P5C) (Hu et al., 1992; Szabados & Savoure, 2010). Ornithine is also catalyzed into P5C by ornithine aminotransferase, and then it is reduced to proline in the cytosol by pyrroline-5-carboxylate reductase (Anwar et al., 2018). Given these observations, we propose that this route is mainly responsible for biosynthesis and accumulation of proline in the response of *K. caspia* to salt stress.

Polyamines (PAs) are small aliphatic nitrogenous bases with two or more amino groups that include putrescine, spermidine, and spermine and are widely distributed in plant species (Liu et al., 2020). In PA biosynthesis, arginine/ornithine can be catalyzed to putrescine by arginine decarboxylase/ornithine decarboxylase. Subsequently, spermidine and spermine are synthesized by sequential additions of aminopropyl groups to putrescine and spermidine, respectively, by the concerted action of spermidine synthase/s-adenosylmethiomine decarboxylase and spermine synthase (Sánchez-Rodríguez et al., 2016). In our study, we showed that salt stress upregulated the expression of *SAMS* and *SMS* and the corresponding metabolites: s-adenosylmethiomine and spermine, respectively (Figure 6C). These data suggested that the spermine biosynthesis route could be dependent on the substrate s-adenosylmethiomine and related to PA biosynthetic enzymes. The accumulation of spermine is regarded as an important indicator of salt tolerance in plants (Maiale et al., 2004), where it acts as a signaling molecule leading to the activation of antioxidant enzymes (Liu et al., 2015; Seifi & Shelp, 2019). Spermine would therefore contribute to the ROS homeostasis in salt-treated *K. caspia* by improving the activity of antioxidant enzymes (Table 1). Elevated spermine is also regarded as one of the most effective osmoprotectants against salt stress (Paul & Roychoudhury, 2016). This would align with the low osmotic potential and high turgor pressure in salt-treated *K. caspia* leaves, which appeared to be associated with the accumulation of organic osmolytes (saccharides/proline/spermine) (Figures 2D–F and 3). The increased SA hints in its roleas an important regulator of salt responses in *K. caspia* (Figure 3). SA can increase polyamine content under salt stress and this has been linked to increased salt tolerance in tomato (Szepesi et al., 2009) and *Medicago sativa* (Palma et al., 2013). SA can also increase Na^+ levels in leaves as well as suppressing ROS (Gémes et al., 2011). The roles of SA in salt responses in recretohalophytes have not been extensively explored, although one report suggests that SA down-regulation in *Aeluropus lagopoides* was important for salt tolerance (Paidi et al., 2017). This did not tally with the increases seen upon salt treatment in *K. caspia*, further work is needed to assess the role of SA in this species. To aid to the comprehension, the proposed role of saccharide metabolism and proline/spermine biosynthesis in *K. caspia* subjected to salt is summarized in Figure 8.

4.2 | Role of TCA cycle in modulating energy balance in *K. caspia* under salt stress

Increased respiratory generation of energy is a survival strategy for plants to adapt to various stressful environments (Chen et al., 2019).

Energy production requires the coordination of several metabolic processes, including glycolysis and the oxidative pentose phosphate pathway in the cytoplasm/plastid and the mitochondrial TCA cycle (Bandehagh & Taylor, 2020). The increase in the glycolysis metabolites glyceraldehyde-3p, PEP and associated gene expression with salt treatment (Figure 6A) suggests that elevated bioenergetic metabolism was also a feature of the salt response in *K. caspia*. However, this need not be a beneficial feature as it could be linked to the enhanced production of ROS (Tiwari et al., 2002). Thus, enhancing the accumulation of glycolysis metabolites could be coupled with the generation of ROS in *K. caspia*.

Glycolysis feeds into the TCA cycle to drive ATP synthesis via the oxidation of respiratory substrates (Sweetlove et al., 2010). Elevated TCA cycle activity has been shown to improve the salt tolerance of wild soybean and Kentucky bluegrass by increasing the energy capacity and the levels of intermediate products under alkaline-salt stress (Hu et al., 2014; Li et al., 2017). However, other literatures have suggested that the concentrations of TCA-cycle intermediates are lower with salt stress, for example, in maize hybrids (Richter et al., 2015). Indeed, the salt-sensitive genotype of Tibetan wild barley (XZ169) consumed more energy in the TCA cycle than the tolerant genotype (XZ26) (Shen et al., 2016). Such discrepancies suggest that the role of the TCA cycle in responses to salt stress should be considered separately in each species. In *K. caspia*, a reduction in most of the intermediates associated with the TCA cycle was observed under salt stress, including fumarate, malate, oxalosuccinate, 2-oxoglutarate, pyruvate, and succinate (Figure 3). Such changes could indicate that *K. caspia* adopts an energy conservation strategy, where there is a transition from plant growth to the induction of protective mechanisms and protein synthesis under salt stress (Liu & Howell, 2010), although this does not appear to be reflected in our measurements of RGR (Figure 1D). Another important clue could be that high salinity had no impact on H_2O_2 content compared with the unstressed plants (Table 1). Therefore, the low level of TCA cycle flux may partially counteract glycolysis-associated ROS overproduction in responses of *K. caspia* to salt (Bandehagh & Taylor, 2020). However, it should be noted that TCA metabolism associated with citrate accumulation was actually increased in *K. caspia* (Figure 3). Citrate accumulation has been linked to the maintenance of pH homeostasis in *Puccinellia tenuiflora* under alkaline stress (Shi et al., 2002); it might be playing a similar role in salt tolerance in *K. caspia*. These hypothesized roles are included in Figure 8.

4.3 | The contribution of hexokinase and polyamine transporter to ions homeostasis in *K. caspia* under salt stress

Hexokinase is a sensor for the glycolysis of D-glucose to modulate saccharides utilization in planta (Li et al., 2018). We observed that salt stress upregulated *HEXOKINASE* and glucose in leaves of *K. caspia* (Figure 6B). Interestingly, the apple glucose sensor MdHXK1 (HEXOKINASE1) could interact with and phosphorylate MdNHX1
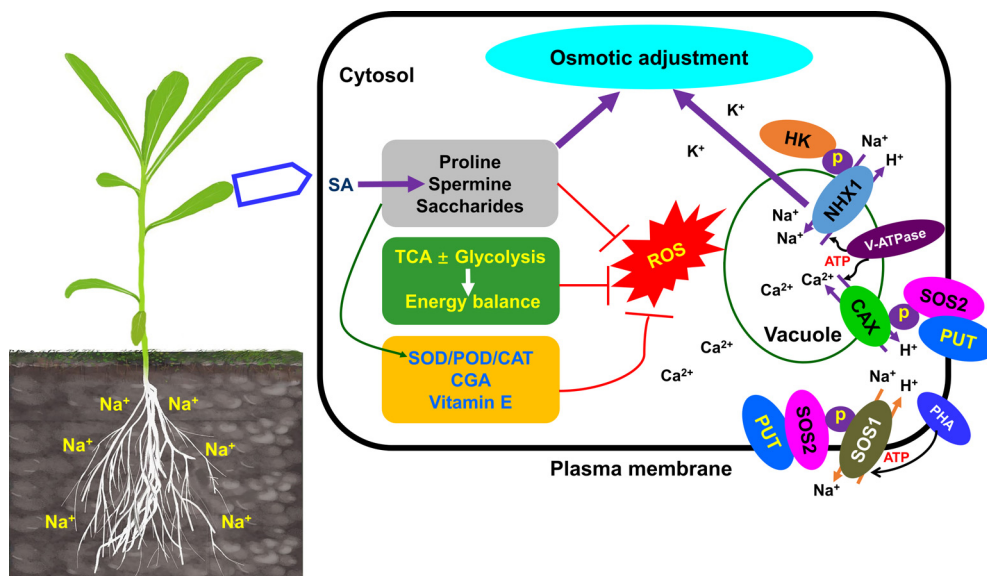
FIGURE 8 Schematic model of osmotic adjustment, ROS scavenging, and ions homeostasis in leaf cells of *K. caspia* treated with salt. In the presence of salt, (1) organic osmolytes, such as proline, spermine, and saccharides increase dramatically. HK phosphorylated NHX1 to promote the sequestration of cytoplasmic Na^+ into vacuoles. Both organic osmolytes and inorganic ions contribute to osmotic adjustment to reduce cellular osmotic potential and improve turgor pressure. (2) Accumulation of organic osmolytes and elevated salicylic acid could indirectly enhance the antioxidant enzyme activities (SOD/POD/CAT) to reduce the excess ROS. The accumulation of CGA and vitamin E will also scavenge ROS. In addition to this, low TCA cycle flux may counteract glycolysis-associated energy consumption to suppress ROS overproduction. (3) PUT might be involved in recruiting and activating SOS2 at the plasma membrane to facilitate the transport activity of SOS1 and CAX to extrude Na^+ into the apoplast and sequestrate Ca^{2+} into vacuoles, respectively, thereby modulating ions homeostasis

(Na^+/H^+ EXCHANGER 1) to transport the intracellular Na^+ into vacuoles to maintain the ion homeostasis under salt stress (Sun et al., 2018). Previous studies showed that the expression of *KcNHX1* was induced and regulated by salt stress, which is responsible for sequestering Na^+ into leaf vacuoles (Guo et al., 2020b; Liu et al., 2012). If the precedent established with the apple glucose sensor MdHXK1 is valid for *K. caspia* (Sun et al., 2018), we speculate that the hexokinase-NHX1 regulatory module might contribute to maintain Na^+ homeostasis in *K. caspia* in response to salt. In addition to this, salt-treated plants could enhance the level of spermine to alter Ca^{2+} allocation to modulate Ca^{2+} homeostasis (Yamaguchi et al., 2006). The SALT OVERLY SENSITIVE 2 (SOS2) protein kinase also specifically activates the tonoplast Ca^{2+}/H^+ antiporter CAX1 that is involved in Ca^{2+} homeostasis under salt stress (Cheng et al., 2004). Such observations suggest that polyamines (PAs), especially spermine, might have regulatory links between protein kinase and ion transporters in plants subjected to salt stress. Furthermore, our data showed that salt upregulated the transcription of *PUT* (plasma membrane polyamine transporter gene)/*CAX/SOS1/SOS2* (data not shown) and *SRM*, accompanied by the increase in spermine and Na^+ concentration but no impact on the concentrations of K^+ and Ca^{2+} in leaves (Figures 2A and 6C). Notably, a recent report in *Arabidopsis* indicated that the PUT3-SOS1-SOS2 complex could not only modulate SOS1-mediated Na^+ efflux to reduce cytosolic Na^+ concentrations but also activate PUT3 to promote the accumulation of PAs to protect cells from oxidative damage (Chai et al., 2020). Our previous findings showed that KcSOS1 participated in the process of Na^+ secretion to

maintain K^+/Na^+ homeostasis at a whole plant level (Guo et al., 2020b). Based on such evidence, we cannot rule out that PUT might recruit and activate SOS2 at the plasma membrane to facilitate the transport activity of SOS1 and CAX, further modulating ions homeostasis in *K. caspia* under salt conditions (Figure 8). However, these hypotheses will need to be confirmed by further research.

4.4 | Chlorogenic acid/vitamin E biosynthesis may be involved in the maintenance of ROS homoeostasis in *K. caspia* under salt stress

Chlorogenic acid (CGA) is an antioxidant phenolic acid that can aid the prevention of cardiovascular disease and other age-related diseases (Meinhart et al., 2019). The CGA biosynthesis pathway is defined in different plant species (Clifford et al., 2017). Besides the better-established route based on shikimate, another pathway is based on hydroxycinnamoyl-CoA: quinate hydroxycinnamoyl transferases (HQT) prefers to use quinate as an acyl acceptor (Kriegshauser et al., 2021). Suppressing HQT leads to a dramatic reduction in CGA content (by 98%) in *Nicotiana benthamiana*, demonstrating that HQT is directly involved in CGA biosynthesis (Niggeweg et al., 2004; Sonnante et al., 2010). Other literature also proved that HQT2 is the last rate-limiting enzyme controlling the production of CGA in *Taraxacum antungense* (Liu et al., 2019). In line with such reports, we observed that the upregulation of *HQT* expression correlated with the accumulation of CGA and its precursor in *K. caspia* subjected to salt

stress (Figure 6D). In addition to this, increases in AtHQT orthologous hydroxycinnamoyl-CoA, shikimate/quinate hydroxycinnamoyl transferases (AtHCT), were noted. HCT also has a broad acceptor substrate range (Hoffmann et al., 2003; Sander & Petersen, 2011) and has been mainly linked to lignin biosynthesis and composition (Hoffmann et al., 2004). However, HCT2 has also been associated with CGA biosynthesis in *Cecropia obtusifolia* and *Populus*. In the latter, HCT2 is involved in the defense response via the WRKY transcriptional regulatory pathway (Cadena-Zamudio et al., 2020; Zhang et al., 2018). Based on these observations, we suggest that HQT or HCT is a key enzyme that may recognize an acyl acceptor, quinic acid or shikimic acid to determine CGA biosynthesis in salt-treated *K. caspia* (Figure 7). Meanwhile, the accumulation of CGA could be linked to the maintenance of redox homeostasis under salt stress (Kiani et al., 2021). As our data showed that ROS levels are unchanged in *K. caspia* exposed to salt (Table 1), it may be fulfilling a similar role here.

Vitamin E, a potent lipid-soluble antioxidant protecting cell membranes from free radical damage is also a relevant compound of the oxidative homeostasis (Muñoz & Munné-Bosch, 2019). We observed the up-regulation upon salt treatment of a key gene *HPPD* (*HYDROXYPHENYL PYRUVATE DIOXYGENASE*) involved in vitamin E biosynthesis as well as the content of important intermediates of the biosynthetic pathway: 4-hydroxyphenylpyruvate (HPP) and homogentisate (HGA) (Figure 6E). HPP derives from tyrosine degradation (Riewe et al., 2012) and is then converted into HGA by the enzymatic action of HPPD (Mène-Saffrané & Pellaud, 2017). HGA and phytyl diphosphate (PDP) are condensed into the intermediate methylphytyl benzoquinone (MPBQ) by the homogentisate phytyl transferase (HPT) enzyme (Chen et al., 2006). HPT is one of the most important enzymes catalyzing the later steps of the vitamin E biosynthetic pathway along with γ-TMT (Shintani & DellaPenna, 1998). In line with this, the expression of *γ-TMT* was positively correlated with the accumulation of γ-tocopherol in *K. caspia* under salt stress (Figure 6E), implying its importance in the salt response. This was supported by recent research showing that co-overexpression of *AtHPT* and *Atγ-TMT* enhances the α-tocopherols content and cellular antioxidant enzyme activity, hence improving salt and cadmium tolerance in potato (Upadhyaya et al., 2021). The likely important role of the end product α-tocopherol content in vitamin E biosynthetic pathway in conferring protection from oxidative damage in *K. caspia* under salt stress is included in Figure 8.

5 | CONCLUSIONS

Our present study demonstrated that the adaptation of *K. caspia* to soil salinity may be modulated at transcriptomic and metabolomic levels. Some of these primary metabolites (saccharides, TCA intermediates, proline, and spermine) and key secondary metabolites (CGA and vitamin E) were closely associated with the transcriptional levels of genes coding for enzymes participating in fundamental biological processes during salinity stress. Notably, at transcriptional and metabolic levels, the key genes and metabolites linked to saccharide metabolism, TCA cycle, proline/spermine

biosynthesis and CGA/vitamin E biosynthesis might facilitate the osmotic adjustment and remove the excess ROS in *K. caspia* under salt conditions. Therefore, our findings provide novel insights for understanding the inter-coordination of multiple metabolic pathways that contribute to the adaption of *K. caspia* to saline environments.

AUTHOR CONTRIBUTIONS

Luis A. J. Mur, Juying Wu, and Qiang Guo conceived and designed this research. Qiang Guo, Jiwan Han, Cui Li, Chunqiao Zhao, Qinghai Wang, and Xincun Hou performed the experiments. Qiang Guo and Jiwan Han carried out data analysis. Qiang Guo wrote the manuscript. Luis A. J. Mur reviewed and edited the manuscript. We declare no conflicts of interest in relation to this study.

DATA AVAILABILITY STATEMENT

The data that support the findings of this study are openly available in NCBI Sequence Read Archive database (accession number: PRJNA744046).

ORCID

Qiang Guo https://orcid.org/0000-0001-5361-9294
Qinghai Wang https://orcid.org/0000-0002-6230-9068
Luis A. J. Mur https://orcid.org/0000-0002-0961-9817

REFERENCES

Anwar, A., She, M., Wang, K., Riaz, B. & Ye, X. (2018) Biological roles of ornithine aminotransferase (OAT) in plant stress tolerance: present progress and future perspectives. *International Journal of Molecular Sciences*, 19, 3681.

Bandehagh, A. & Taylor, N.L. (2020) Can alternative metabolic pathways and shunts overcome salinity induced inhibition of central carbon metabolism in crops? *Frontiers in Plant Science*, 11, 1072.

Baptista, R., Fazakerley, D.M., Beckmann, M., Baillie, L. & Mur, L.A.J. (2018) Untargeted metabolomics reveals a new mode of action of pretomanid (PA-824). *Scientific Reports*, 8, 5084.

Beckmann, M., Parker, D., Enot, D.P., Duval, E. & Drape, J. (2008) High-throughput, nontargeted metabolite fingerprinting using nominal mass flow injection electrospray mass spectrometry. *Nature Protocols*, 3, 486–504.

Blande, D., Halimaa, P., Tervahauta, A.I., Aarts, M.G.M. & Kärenlampi, S.O. (2017) De novo transcriptome assemblies of four accessions of the metal hyperaccumulator plant *Noccaea caerulescens*. *Scientific Data*, 4, 160131.

Cadena-Zamudio, J.D., Nicasio-Torres, P., Monribot-Villanueva, J.L., Guerrero-Analco, J.A. & Ibarra-Laclette, E. (2020) Integrated analysis of the transcriptome and metabolome of *Cecropia obtusifolia*: a plant with high chlorogenic acid content traditionally used to treat diabetes mellitus. *International Journal of Molecular Sciences*, 21, 7572.

Chai, H.X., Guo, J.F., Zhong, Y.L., Hsu, C.C., Zou, C.S., Wang, P.C. et al. (2020) The plasma-membrane polyamine transporter PUT3 is regulated by the Na⁺/H⁺ antiporter SOS1 and protein kinase SOS2. *New Phytologist*, 226, 785–797.

Chen, J., Le, X.C. & Zhu, L.Z. (2019) Metabolomics and transcriptomics reveal defense mechanism of rice (*Oryza sativa*) grains under stress of 2, 2′, 4, 4′-tetrabromodiphenyl ether. *Environment International*, 133, 105154.

Chen, S., Li, H. & Liu, G. (2006) Progress of vitamin E metabolic engineering in plants. *Transgenic Research*, 15, 655–665.

Cheng, N.H., Pittman, J.K., Zhu, K. & Hirsch, K.D. (2004) The protein kinase SOS2 activates the *Arabidopsis* H⁺/Ca²⁺ antiporter CAX1 to integrate calcium transport and salt tolerance. *Journal of Biological Chemistry*, 279, 2922–2926.

Clifford, M.N., Jaganath, I.B., Ludwig, I.A. & Crozier, A. (2017) Chlorogenic acids and the acyl-quinic acids: discovery, biosynthesis, bioavailability and bioactivity. *Natural Product Reports*, 34, 1391–1421.

Cui, Y.N., Li, X.T., Yuan, J.Z., Wang, F.Z., Guo, H., Xia, Z.R. et al. (2020) Chloride is beneficial for growth of the xerophyte *Pugionium cornutum* by enhancing osmotic adjustment capacity under salt and drought stresses. *Journal of Experimental Botany*, 71, 4215–4231.

Dong, Y.P., Fan, G.Q., Zhao, Z.L. & Deng, M.J. (2014) Transcriptome expression profiling in response to drought stress in *Paulownia australis*. *International Journal of Molecular Sciences*, 15, 4583–4607.

Elbein, A.D., Pan, Y.T., Pastuszak, I. & Carroll, D. (2003) New insights on trehalose: a multifunctional molecule. *Glycobiology*, 13, 17R–27R.

Fisher, L.H., Han, J., Corke, F.M., Akinyemi, A., Didion, T., Nielsen, K.K. et al. (2016) Linking dynamic phenotyping with metabolite analysis to study natural variation in drought responses of *Brachypodium distachyon*. *Frontiers in Plant Science*, 7, 1751.

Flowers, T.J. & Colmer, T.D. (2008) Salinity tolerance in halophytes. *New Phytologist*, 179, 945–963.

Flowers, T.J., Munns, R. & Colmer, T.D. (2015) Sodium chloride toxicity and the cellular basis of salt tolerance in halophytes. *Annals of Botany*, 115, 419–431.

Flowers, T.J. & Muscolo, A. (2015) Introduction to the special issue: halophytes in a changing world. *AoB Plants*, 7, plv020.

Gao, Y.L., Li, M.N., Zhang, X.X., Yang, Q.C. & Huang, B.R. (2020) Upregulation of lipid metabolism and glycine betaine synthesis are associated with choline-induced salt tolerance in halophytic *seashore paspalum*. *Plant Cell & Environment*, 43, 159–173.

Gémes, K., Poór, P., Horváth, E., Kolbert, Z., Szopkó, D., Szepesi, A. et al. (2011) Cross-talk between salicylic acid and NaCl-generated reactive oxygen species and nitric oxide in tomato during acclimation to high salinity. *Physiolgia Plantarum*, 142, 179–192.

Ghahremani, M., Ghanati, F., Bernard, F., Azad, T., Gholami, M. & Safari, M. (2014) Ornithine-induced increase of proline and polyamines contents in tobacco cells under salinity conditions. *Australian Journal of Crop Science*, 8, 91–96.

González-Orenga, S., Ferrer-Gallego, P.P., Laguna, E., López-Gresa, M.P., Donat-Torres, M.P., Verdeguer, M. et al. (2019) Insights on salt tolerance of two endemic *Limonium* species from Spain. *Metabolites*, 9, 294.

Guo, Q., Meng, L., Han, J.W., Mao, P.C., Tian, X.X., Zheng, M.L. et al. (2020b) SOS1 is a key systemic regulator of salt secretion and K⁺/Na⁺ homeostasis in the recretohalophyte *Karelinia caspia*. *Environmental and Experimental Botany*, 177, 104098.

Guo, Q., Meng, L., Zhang, Y.N., Mao, P.C., Tian, X.X., Li, S.S. et al. (2017) Antioxidative systems, metal ion homeostasis and cadmium distribution in *Iris lactea* exposed to cadmium stress. *Ecotoxicology and Environmental Safety*, 139, 50–55.

Guo, Q., Tian, X.X., Mao, P.C. & Meng, L. (2020a) Overexpression of *Iris lactea* tonoplast Na⁺/H⁺ antiporter gene *IlNHX* confers improved salt tolerance in tobacco. *Biologia Plantarum*, 64, 50–57.

He, J.B., Niu, Y.F., Chen, W.R., Li, J.X., Wang, L.B., Zi, T.P. et al. (2016) Chemical constituents from *Karelinia caspia*. *Chinese Traditional Patent Medicine*, 38, 1062–1066 (in Chinese).

Hoffmann, L., Besseau, S., Geoffroy, P., Ritzenthaler, C., Meyer, D., Lapierre, C. et al. (2004) Silencing of hydroxycinnamoyl-coenzyme A shikimate/quinate hydroxycinnamoyltransferase affects phenylpropanoid biosynthesis. *The Plant Cell*, 16, 1446–1465.

Hoffmann, L., Maury, S., Martz, F., Geoffroy, P. & Legrand, M. (2003) Purification, cloning, and properties of an acyltransferase controlling shikimate and quinate ester intermediates in phenylpropanoid metabolism. *Journal of Biological Chemistry*, 278, 95–103.

Hu, C., Delauney, A.J. & Verma, D. (1992) A bifunctional enzyme (delta 1-pyrroline-5-carboxylate synthetase) catalyzes the first two steps in proline biosynthesis in plants. *Proceedings of the National Academy of Sciences of the United States of America*, 89, 9354–9358.

Hu, L.X., Zhang, P.P., Jiang, Y. & Fu, J.M. (2014) Metabolomic analysis revealed differential adaptation to salinity and alkalinity stress in Kentucky bluegrass (*Poa pratensis*). *Plant Molecular Biology Reporter*, 33, 56–68.

Iordachescu, M. & Imai, R. (2008) Trehalose biosynthesis in response to abiotic stresses. *Journal of Integrative Plant Biology*, 50, 1223–1229.

Isayenkov, S.V. & Maathuis, F.J.M. (2019) Plant salinity stress: many unanswered questions remain. *Frontiers in Plant Science*, 10, 80.

Jin, S.X. & Daniell, H. (2014) Expression of γ-tocopherol methyltransferase in chloroplasts results in massive proliferation of the inner envelope membrane and decreases susceptibility to salt and metal-induced oxidative stresses by reducing reactive oxygen species. *Plant Biotechnology Journal*, 12, 1274–1285.

Kiani, R., Arzani, A. & Mirmohammady Maibody, S.A.M. (2021) Polyphenols, flavonoids, and antioxidant activity involved in salt tolerance in wheat, *Aegilops cylindrica* and their smphidiploids. *Frontiers in Plant Science*, 12, 646221.

Kiani-Pouya, A., Roessner, U., Jayasinghe, N.S., Lutz, A., Rupasinghe, T., Bazihizina, N. et al. (2017) Epidermal bladder cells confer salinity stress tolerance in the halophyte quinoa and *Atriplex* species. *Plant Cell & Environment*, 40, 1900–1915.

Kriegshauser, L., Knosp, S., Grienenberger, E., Tatsumi, K., Gütle, D.D., Sørensen, I. et al. (2021) Function of the hydroxycinnamoyl-CoA: shikimate hydroxycinnamoyl transferase is evolutionarily conserved in embryophytes. *The Plant Cell*, 33, 1472–1491.

Li, B. & Dewey, C.N. (2011) RSEM: accurate transcript quantification from RNA-seq data with or without a reference genome. *BMC Bioinformatics*, 12, 93–99.

Li, K.L., Chen, J. & Zhu, L.Z. (2018) The phytotoxicities of decabromodiphenyl ether (BDE-209) to different rice cultivars (*Oryza sativa* L.). *Environmental Pollution*, 235, 692–699.

Li, M.X., Guo, R., Jiao, Y., Jin, X.F., Zhang, H.Y. & Shi, L.X. (2017) Comparison of salt tolerance in Soja based on metabolomics of seedling roots. *Frontiers in Plant Science*, 8, 1–16.

Li, X., Ma, X.D., Cheng, Y.H., Liu, J.X., Zou, J.Z., Zhai, F.F., Sun, Z.Y. & Han, L. (2021) Transcriptomic and metabolomic insights into the adaptive response of *Salix viminalis* to phenanthrene. *Chemosphere*, 262, 127573.

Liao, L., Dong, T.T., Qiu, X., Rong, Y., Sun, G.C., Wang, Z.H. et al. (2019) Antioxidant enzyme activity and growth responses of Huangguogan citrus cultivar to nitrogen supplementation. *Bioscience, Biotechnology, and Biochemistry*, 83, 1924–1936.

Liu, J.H., Wang, W., Wu, H., Gong, X. & Moriguchi, T. (2015) Polyamines function in stress tolerance: from synthesis to regulation. *Frontiers in Plant Science*, 6, 827.

Liu, J.L., Yang, R.C., Jian, N., Wei, L., Ye, L.L., Wang, R.H. et al. (2020) Putrescine metabolism modulates the biphasic effects of

brassinosteroids on canola and Arabidopsis salt tolerance. *Plant Cell & Environment*, 43, 1348–1359.

Liu, J.X. & Howell, S.H. (2010) Endoplasmic reticulum protein quality and its relationship to environmental stress responses in plants. *The Plant Cell*, 22, 2930–2942.

Liu, L., Zeng, Y., Pan, X. & Zhang, F. (2012) Isolation, molecular characterization, and functional analysis of the vacuolar Na^+/H^+ antiporter genes from the halophyte *Karelinia caspica*. *Molecular Biology Reports*, 39, 7193–7202.

Liu, Q., Yao, L.X., Xu, Y.C., Cheng, H.T., Wang, W.T., Liu, Z.J. et al. (2019) In vitro evaluation of hydroxycinnamoyl CoA: quinate hydroxycinnamoyl transferase expression and regulation in *Taraxacum antungense* in relation to 5-caffeoylquinic acid production. *Phytochemistry*, 162, 148–156.

Love, M., Huber, W. & Anders, S. (2014) Moderated estimation of fold change and dispersion for RNA-seq data with DESeq2. *Genome Biology*, 15, 550.

Ma, Q., Yue, L.J., Zhang, J.L., Wu, G.Q., Bao, A.K. & Wang, S.M. (2012) Sodium chloride improves photosynthesis and water status in the succulent xerophyte *Zygophyllum xanthoxylum*. *Tree Physiology*, 32, 4–13.

Maiale, S., Sánchez, D.H., Guirado, A., Vidal, A. & Ruiz, O.A. (2004) Spermine accumulation under salt stress. *Journal of Plant Physiology*, 161, 35–42.

Martínez, J.P., Kinet, J.M., Bajji, M. & Lutts, S. (2005) NaCl alleviates polyethylene glycol induced water stress in the halophyte species *Atriplex halimus* L. *Journal of Experimental Botany*, 419, 2421–2431.

Meinhart, A.D., Damin, F.M., Caldeirão, L., de Jesus Filho, M., da Silva, L.C., da Silva Constant, L. et al. (2019) Chlorogenic and caffeic acids in 64 fruits consumed in Brazil. *Food Chemistry*, 286, 51–63.

Mène-Saffrané, L. & Pellaud, S. (2017) Current strategies for vitamin E biofortification of crops. *Current Opinion in Biotechnology*, 44, 189–197.

Munns, R., James, R.A., Xu, B. et al. (2012) Wheat grain yield on saline soils is improved by an ancestral Na^+ transporter gene. *Nature Biotechnology*, 30, 360–364.

Munns, R. & Tester, M. (2008) Mechanisms of salinity tolerance. *Annual Review of Plant Biology*, 59, 651–681.

Muñoz, P. & Munné-Bosch, S. (2019) Vitamin E in plants: biosynthesis, transport, and function. *Trends in Plant Science*, 24, 1040–1051.

Niggeweg, R., Michael, A.J. & Martin, C. (2004) Engineering plants with increased levels of the antioxidant chlorogenic acid. *Nature Biotechnology*, 2, 746–754.

Paes de Araújo, R., Bertoni, N., Seneda, A., Felix, T., Carvalho, M., Lewis, K. et al. (2019) Defining metabolic rewiring in lung squamous cell carcinoma. *Metabolites*, 9, 47.

Paidi, M.K., Agarwal, P., More, P. & Agarwal, P.K. (2017) Chemical derivatization of metabolite mass profiling of the recretohalophyte *Aeluropus lagopoides* revealing salt stress tolerance mechanism. *Marine Biotechnology (NY)*, 19, 207–218.

Palma, F., López-Gómez, M., Tejera, N.A. & Lluch, C. (2013) Salicylic acid improves the salinity tolerancre of *Medicago sativa* in symniosis with *Sinorhizobium meliloti* by preventing nitrogen fixation inhibition. *Plant Science*, 208, 75–82.

Pang, Z.Q., Chong, J., Zhou, G.Y., de Lima Morais, D.A., Chang, L., Barrette, M. et al. (2021) MetaboAnalyst 5.0: narrowing the gap between raw spectra and functional insights. *Nucleic Acids Research*, 49, W388–W396.

Paul, S. & Roychoudhury, A. (2016) Seed priming with spermine ameliorates salinity stress in the germinated seedlings of two rice cultivars differing in their level of salt tolerance. *Tropical Plant Research*, 3, 616–633.

Richter, J.A., Erban, A., Kopka, J. & Zörb, C. (2015) Metabolic contribution to salt stress in two maize hybrids with contrasting resistance. *Plant Science*, 233, 107–115.

Riewe, D., Koohi, M., Lisec, J., Pfeiffer, M., Lippmann, R., Schmeichel, J. et al. (2012) A tyrosine aminotransferase involved in tocopherol synthesis in *Arabidopsis*. *The Plant Journal*, 71, 850–859.

Sánchez-Rodríguez, E., Romero, L. & Ruiz, J.M. (2016) Accumulation of free polyamines enhances the antioxidant response in fruits of grafted tomato plants under water stress. *Journal of Plant Physiology*, 190, 72–78.

Sander, M. & Petersen, M. (2011) Distinct substrate specificities and unusual substrate flexibilities of two hydroxycinnamoyltransferases, rosmarinic acid synthase and hydroxycinnamoyl-CoA:shikimate hydroxycinnamoyl-transferase, from *Coleus blumei* Benth. *Planta*, 233, 1157–1171.

Sarker, U. & Oba, S. (2018) Augmentation of leaf color parameters, pigments, vitamins, phenolic acids, flavonoids and antioxidant activity in selected *Amaranthus tricolor* under salinity stress. *Scientific Reports*, 8, 12349.

Seifi, H.S. & Shelp, B.J. (2019) Spermine differentially refines plant defense responses against biotic and abiotic stresses. *Frontiers in Plant Science*, 10, 117.

Shabala, S. (2013) Learning from halophytes: physiological basis and strategies to improve abiotic stress tolerance in crops. *Annals of Botany*, 112, 1209–1221.

Shabala, S., Bose, J. & Hedrich, R. (2014) Salt bladders: do they matter? *Trends in Plant Science*, 19, 687–691.

Sharma, D.K., Andersen, S.B., Ottosen, C.O. & Rosenqvist, E. (2015) Wheat cultivars selected for high Fv/Fm under heat stress maintain high photosynthesis, total chlorophyll, stomatal conductance, transpiration and dry matter. *Physiologia Plantarum*, 153, 284–298.

Shen, Q.F., Fu, L.B., Dai, F., Jiang, L.X., Zhang, G.P. & Wu, D.Z. (2016) Multi-omics analysis reveals molecular mechanisms of shoot adaption to salt stress in Tibetan wild barley. *BMC Genomics*, 17, 889.

Shi, D.C., Yin, S., Yang, G. & Zhao, K. (2002) Citric acid accumulation in an alkali-tolerant plant *Puccinellia tenuiflora* under alkaline stress. *Acta Botanica Sinica*, 44, 537–540.

Shintani, D. & DellaPenna, D. (1998) Elevating the vitamin E content of plants through metabolic engineering. *Science*, 282, 2098–2100.

Singh, S.K., Barnaby, J.Y., Reddy, V.R. & Sicher, R.C. (2016) Varying response of the concentration and yield of soybean seed mineral elements, carbohydrates, organic acids, amino acids, protein, and oil to phosphorus starvation and CO_2 enrichment. *Frontiers in Plant Science*, 7, 1967.

Sirin, S. & Aslım, B. (2019) Determination of antioxidant capacity, phenolic acid composition and antiproliferative effect associated with phenylalanine ammonia lyase (PAL) activity in some plants naturally growing under salt stress. *Medicinal Chemistry Research*, 28, 229–238.

Slama, I., Abdelly, C., Bouchereau, A., Flowers, T. & Savouré, A. (2015) Diversity, distribution and roles of osmoprotective compounds accumulated in halophytes under abiotic stress. *Annals of Botany*, 15, 433–447.

Song, J. & Wang, B. (2014) Using euhalophytes to understand salt tolerance and to develop saline agriculture: *Suaeda salsa* as a promising model. *Annals of Botany*, 115, 541–553.

Sonnante, G., D'Amore, R., Blanco, E., Pierri, C.L., De Palma, M., Luo, J. et al. (2010) Novel hydroxycinnamoyl-coenzyme a quinate transferase genes from artichoke are involved in the synthesis of chlorogenic acid. *Plant Physiology*, 153, 1224–1238.

Sun, M.H., Ma, Q.J., Hu, D.G., Zhu, X.P., You, C.X., Shu, H.R. et al. (2018) The glucose sensor MdHXK1 phosphorylates a tonoplast Na^+/H^+ exchanger to improve salt tolerance. *Plant Physiology*, 176, 2977–2990.

Sweetlove, L.J., Beard, K.F.M., Nunes-Nesi, A., Fernie, A.R. & Ratcliffe, R.G. (2010) Not just a circle: flux modes in the plant TCA cycle. *Trends in Plant Science*, 15, 462–470.

Szabados, L. & Savoure, A. (2010) Proline: a multifunctional amino acid. *Trends in Plant Science*, 15, 89–97.

Szepesi, Á., Csiszár, J., Gémes, K., Horváth, E., Horváth, F., Simon, M.L. et al. (2009) Salicylic acid improves acclimation to salt stress by stimulating abscisic aldehyde oxidase activity and abscisic acid

accumulation, and increases Na$^+$ content in leaves without toxicity symptoms in *Solanum lycopersicum* L. *Journal of Plant Physiology*, 166, 914–925.

Tang, X.L., Mu, X.M., Shao, H.B., Wang, H.Y. & Brestic, M. (2015) Global plant-responding mechanisms to salt stress: physiological and molecular levels and implications in biotechnology. *Critical Reviews in Biotechnology*, 35, 425–437.

Tiwari, B.S., Belenghi, B. & Levine, A. (2002) Oxidative stress increased respiration and generation of reactive oxygen species, resulting in ATP depletion, opening of mitochondrial permeability transition, and programmed cell death. *Plant Physiology*, 128, 1271–1281.

Upadhyaya, D.C., Bagri, D.S., Upadhyaya, C.P., Kumar, A., Thiruvengadam, M. & Jain, S.K. (2021) Genetic engineering of potato (*Solanum tuberosum* L.) for enhanced α-tocopherols and abiotic stress tolerance. *Physiologia Plantarum*, 173, 116–128.

Wang, C., Lei, J.Q., Li, S.Y., Mao, D.L., Rahmutulia, Z. & Zhou, J. (2013) Morphological characteristics of *Karelinia caspica* Nebkhas in the oasis-desert ecotone in Cele, Xinjiang, China. *Journal of Desert Research*, 33, 981–989 (In Chinese).

Wang, X., Bai, J.H., Wang, W., Zhang, G.L., Yin, S. & Wang, D.W. (2021) A comparative metabolomics analysis of the halophyte *Suaeda salsa* and *Salicornia europaea*. *Environmental Geochemistry and Health*, 43, 1109–1122.

Xue, J., Bao, Y.Y., Li, B.L., Cheng, Y.B., Peng, Z.Y., Liu, H. et al. (2010) Transcriptome analysis of the brown planthopper *Nilaparvata lugens*. *PLoS One*, 5, e14233.

Yamaguchi, K., Takahashi, Y., Berberich, T., Imai, A., Miyazaki, A., Takahashi, T. et al. (2006) The polyamine spermine protects against high salt stress in *Arabidopsis thaliana*. *FEBS Letters*, 580, 6783–6788.

Yan, K., Zhao, S.J., Bian, L.X. & Chen, X.B. (2017) Saline stress enhanced accumulation of leaf phenolics in honeysuckle (*Lonicera japonica* Thunb.) without induction of oxidative stress. *Plant Physiology and Biochemistry*, 112, 326–334.

Yancey, P.H. (2005) Organic osmolytes as compatible, metabolic and counteracting cytoprotectants in high osmolarity and other stresses. *Journal of Experimental Biology*, 208, 2819–2830.

Yang, L.J., Xie, L.Q., Guo, D.L. & Yan, W.L. (2019b) Chemical constituents from the overground parts of *Karelinia caspia*. *Chinese Traditional Patent Medicine*, 41, 1303–1307 (In Chinese).

Yang, Y., Wu, Y., Ma, L., Yang, Z., Dong, Q., Li, Q. et al. (2019a) The Ca^{2+} sensor SCaBP3/CBL7 modulates plasma membrane H$^+$-ATPase activity and promotes alkali tolerance in *Arabidopsis*. *The Plant Cell*, 31, 1367–1384.

Yuan, H.J., Ma, Q., Wu, G.Q., Wang, P., Hu, J. & Wang, S.M. (2015) ZxNHX controls Na$^+$ and K$^+$ homeostasis at the whole-plant level in *Zygophyllum xanthoxylum* through feedback regulation of the expression of genes involved in their transport. *Annals of Botany*, 115, 495–507.

Zhang, C., Meng, L., Mao, P.C., Tian, X.X. & Guo, Q. (2020) Genetic transformation system construction of *KcSOS1*-RNAi and primary functional identification in halophyte *Karelinia caspia*. *Plant Physiology Journal*, 56, 529–539 (in Chinese).

Zhang, J., Yang, Y., Zheng, K.J. et al. (2018) Genome-wide association studies and expression-based quantitative trait loci analyses reveal roles of HCT2 in caffeoylquinic acid biosynthesis and its regulation by defense responsive transcription factors in *Populus*. *New Phytologist*, 220, 502–516.

Zhang, X., Liao, M., Chang, D. & Zhang, F. (2014) Comparative transcriptome analysis of the Asteraceae halophyte *Karelinia caspica* under salt stress. *BMC Research Notes*, 7, 927.

SUPPORTING INFORMATION

Additional supporting information may be found in the online version of the article at the publisher's website.